

Although a new band is not observed in absorption (as is the case for iodide gegenions),<sup>19</sup> the quenching of P2VP emission (Figure 1) at high  $\beta$  can be attributed to charge-transfer quenching. It is expected that charge-transfer complexes can be destabilized or destroyed by addition of a salt. Indeed, upon addition of  $\text{Na}_2\text{SO}_4$  (Table I) to HCl-containing solutions of P2VP the emission intensity at 390 nm increases. This is explained as the result of the screening of electrostatic repulsions of neighboring protonated rings which relieves the need for gegenion condensation. The sulfate ions are not as effective as chloride ions at forming charge-transfer complexes and at quenching emission of the protonated rings.

It is rather remarkable that EP has no emission at 390 nm or at 350 nm. At HCl concentrations between 1 and  $10^{-7}$  M or in basic solutions, the EP emission is weak in intensity and maximizes at ca. 290 nm. The differences between P2VP and EP can be attributed to cooperative processes in the polymer or to specific local conformations of the monomer units forced by the polymer structure and that cannot be achieved by EP.

### Conclusion

The fluorescence emission properties of aqueous solutions and aqueous/alcohol solutions of P2VP are sensitive to pH changes. At low acidity near neutrality an emission (350 nm) characteristic of hydrogen-bonded pyridine rings is observed and at higher acidities an emission (390 nm) characteristic of protonated pyridine rings is observed. At still higher acidities studied all emission is quenched. Since the absorption spectra of P2VP do not change significantly with corresponding change in acidity, these results are explained in terms of structure features of the electronically excited polymer, in particular its conformation changes and acid-base properties.

**Acknowledgment.** We thank the National Science Foundation, the IBM Corp., and the Army Research Office

for their generous support of the research. I.F.P. thanks the Fullbright Commission for a fellowship.

**Registry No.** P2VP (homopolymer), 25014-15-7; 2-ethylpyridine, 100-71-0.

### References and Notes

- (1) Turro, N. J.; Pierola, I. F., unpublished results.
- (2) Kirsh, Y. E.; Komarova, O. P.; Lukovkin, G. M. *Eur. Polym. J.* 1973, 9, 1405.
- (3) Fuoss, R. M.; Strauss, U. P. *J. Polym. Sci.* 1948, 3, 247.
- (4) Hoover, M. F. *J. Macromol. Sci., Chem. A* 1970, 4, 1324.
- (5) Turro, N. J. "Modern Molecular Photochemistry"; Benjamin/Cummings Publishing Co.: Menlo Park, CA, 1978.
- (6) Forster, T. *Naturwissenschaften* 1949, 36, 186.
- (7) Huppert, D.; Gutman, M.; Kaufmann, K. J. In "Photosensitive Chemistry"; Jortner, J., Levine, R. D., Rice, S. A., Eds.; Wiley-Interscience: New York, 1981; *Adv. Chem. Phys.* No. 47, Part 2, p 643.
- (8) Acuna, A. U.; Catalan, J.; Toribio, F. *J. Phys. Chem.* 1982, 85, 241.
- (9) Catalan, J.; Toribio, F.; Acuna, A. U. *J. Phys. Chem.* 1982, 86, 303.
- (10) Bridges, J. W.; Davies, D. S.; Williams, R. T. *Biochem. J.* 1966, 98, 451.
- (11) Wehry, E. L. In "Practical Fluorescence. Theory, Methods and Techniques"; Guilbault, G. G., Ed.; Marcel Dekker: New York, 1973.
- (12) Konev, S. "Fluorescence and Phosphorescence of Proteins and Nucleic Acids"; Plenum Press: New York, 1967.
- (13) Thomas, J. K.; Almgren, M. In "Solution Chemistry of Surfactants"; Mittal, K. L., Ed.; Plenum Press: New York, 1979; Vol. 2.
- (14) Donck, E. V. *Prog. React. Kinet.* 1970, 5, 273.
- (15) Park, E. H.; Kadhim, A. H.; Offen, H. W. *Photochem. Photobiol.* 1968, 8, 261.
- (16) Weller, A. Z. *Elektrochem.* 1952, 56, 662.
- (17) Forster, T. *Z. Elektrochem.* 1950, 54, 531.
- (18) Morawetz, H. "Macromolecules in Solution"; 2nd ed.; Wiley-Interscience: New York, 1975.
- (19) Kosower, W. M.; Klindinst, P. E. *J. Am. Chem. Soc.* 1956, 78, 3493.
- (20) Turro, N. J.; Tanimoto, Y. *Photochem. Photobiol.* 1981, 34, 173.

## Morphological Studies on the $\alpha$ and $\beta$ Structures of Isotactic Polystyrene

Nancy J. Tyrer and Pudupadi R. Sundararajan\*

Xerox Research Centre of Canada, 2660 Speakman Drive, Mississauga, Ontario L5K 2L1, Canada. Received May 14, 1984

**ABSTRACT:** The morphological features of films of isotactic polystyrene (iPS), crystallized by vapor exposure to hexahydroindan and cyclooctane, are described. Variations in the morphologies with the type of solvent, temperature, and duration of vapor exposure are illustrated. Vapor exposure to hexahydroindan at ambient temperature leads to the crystallization of the  $\beta$  structure with spherulitic morphology. Exposure at 35 °C causes cocrystallization of both  $\alpha$  and  $\beta$  structures. The smaller spherulites corresponding to the  $\alpha$  form appear as overgrowth on the large spherulites of the  $\beta$  structure, resembling a pincushion. Ringed spherulites, corresponding to the  $\beta$  structure, are seen upon exposure of iPS films to cyclooctane vapor at ambient temperature. At above ambient temperatures, e.g., at 27 °C, spherulites with single- and double-armed spirals are obtained. (Here  $\alpha$  refers to the threefold helical structure, and  $\beta$  to the crystalline form with the extended conformation of the chain.)

### Introduction

It has been shown before<sup>1,2</sup> that either the  $\alpha$  (threefold helical) or  $\beta$  (extended conformation) structure or both structures of isotactic polystyrene (iPS) can be crystallized from the bulk, by the technique of solvent-induced crystallization (SINC), with appropriate choice of solvent and

vapor exposure conditions. Although the  $\beta$  structure can be crystallized by the gelation route<sup>3,4</sup> the SINC method offers the advantage of crystallization at room temperature and hence the results are of interest in their own right. The cocrystallization of both  $\alpha$  and  $\beta$  structures from the bulk, by vapor exposure to hexahydroindan and cyclooctane, was described in the previous paper.<sup>2</sup> The equi-

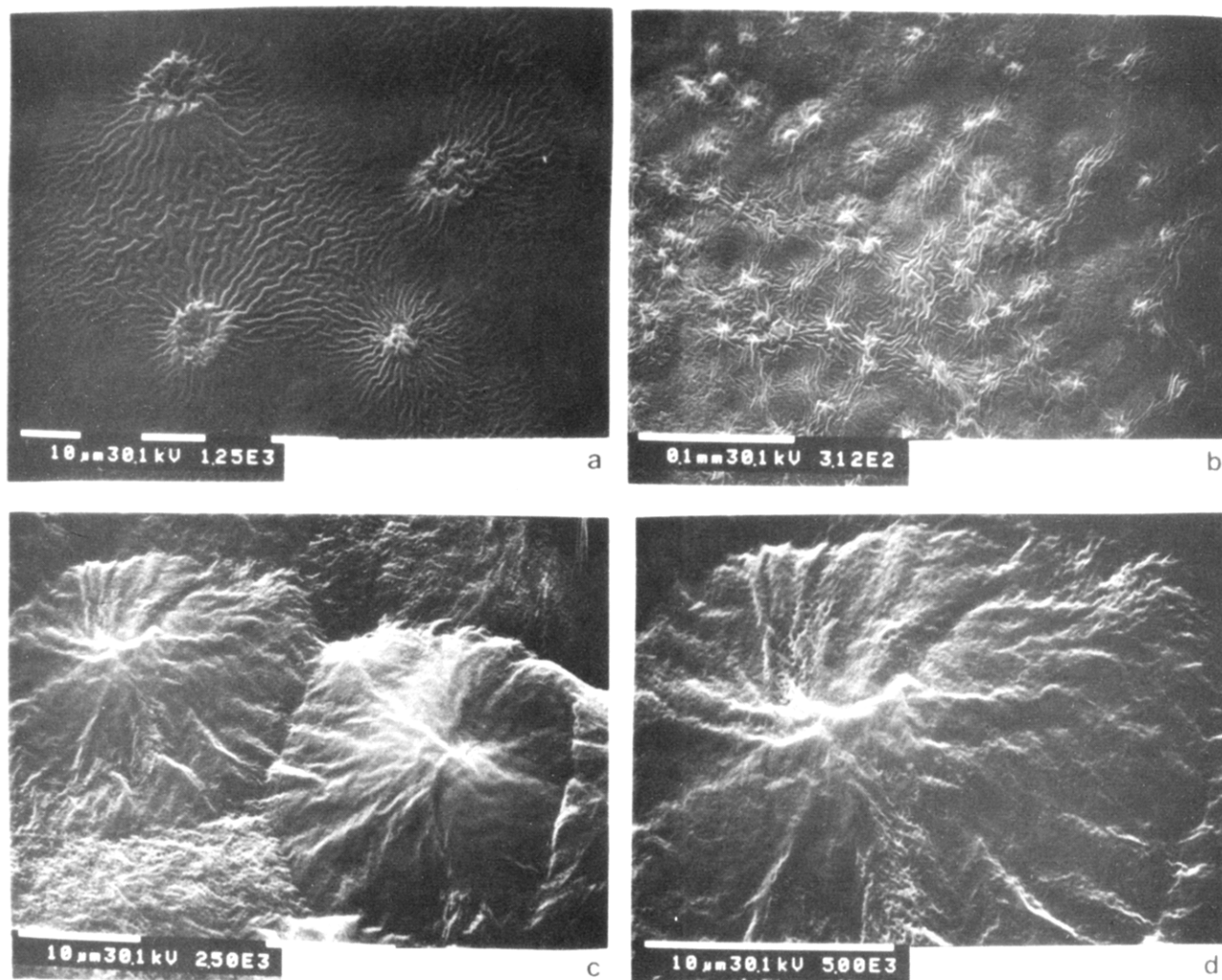


**Figure 1.** Scanning electron micrographs of iPS films exposed to hexahydroindan vapor at ambient temperature for (a) 30, (b) 48, and (c) 68 h. d shows a magnified view of c.

librium crystallinity and disorder parameters corresponding to the two structures were determined quantitatively.

Microscopic studies reported recently<sup>1</sup> showed that the  $\beta$  structure, crystallized from the bulk by SINC, exhibited spherulitic morphology. It is well-known that when two structures are cocrystallized, one acting as a substrate for the other, epitaxy often develops. Overgrowth crystallization in the case of polyethylene has been described by Hill et al.<sup>5</sup> During the growth of lamellar crystals of cellulose II polymorph onto *Valonia* microfibrils (cellulose I), the shish-kebab morphology is seen,<sup>6</sup> with the cellulose II crystals forming the kebab with the microfibrils as the shish. The chain axis of the cellulose II crystals is parallel to that of the microfibrils. Other examples of such epitaxial crystallization are known. Although single-crystal growth of the cellulose type is not involved here, the morphological consequence of cocrystallization of the  $\alpha$  and  $\beta$  forms of iPS would, doubtless, be of interest. This paper describes the morphological studies on iPS films crystallized by solvent vapor exposure, using polarizing optical microscopy (OM), scanning electron microscopy (SEM), small-angle light scattering (SALS), and wide-angle X-ray diffraction (WAXD). The morphological changes in cocrystallized films as a function of time of exposure to solvent vapor were monitored. The development of spherulitic structure associated with the  $\beta$  form is examined in detail. The resultant morphological texture

characteristics using different solvents are compared. A transmission electron microscopic study of the morphology of the gels of iPS has recently been reported by Atkins et al.<sup>7</sup>

### Experimental Section

The sample of iPS used in this study ( $M_w = 250\,360$ ;  $M_n = 62\,900$ ) was obtained from Professor R. W. Lenz (University of Massachusetts) in powder form. It was initially crystalline, in the  $\alpha$  form, as determined by WAXD. Proton NMR analysis (courtesy of Dr. G. K. Hamer of this laboratory), using a Bruker WM250 spectrometer, showed the isotactic dyad content to be 75–80%. The choice of the starting material, different from that described in the previous paper,<sup>2</sup> was dictated by the available quantity. However, studies using this sample have been reported before.<sup>4</sup>

Amorphous films for vapor exposure were prepared by dissolving a melt-quenched sample of iPS (5% w/v) in toluene (ACS grade) and coating the solution onto a glass plate with a mechanical coater and a doctoring blade. The resultant films were stripped from the glass substrate by flotation in water and dried in a vacuum oven at ambient temperature for 24 h. The films were approximately 30  $\mu\text{m}$  thick. The amorphous, unoriented nature of the films was confirmed by WAXD. The film preparation method used here differs from that described in the previous paper.<sup>2</sup> The films used for the crystallinity measurements were about 0.2 mm thick and were unsuitable for optical microscopy and SALS studies. Hence, solution-cast films were used for the present study.

The organic solvents used were spectroscopic-grade ethyl-

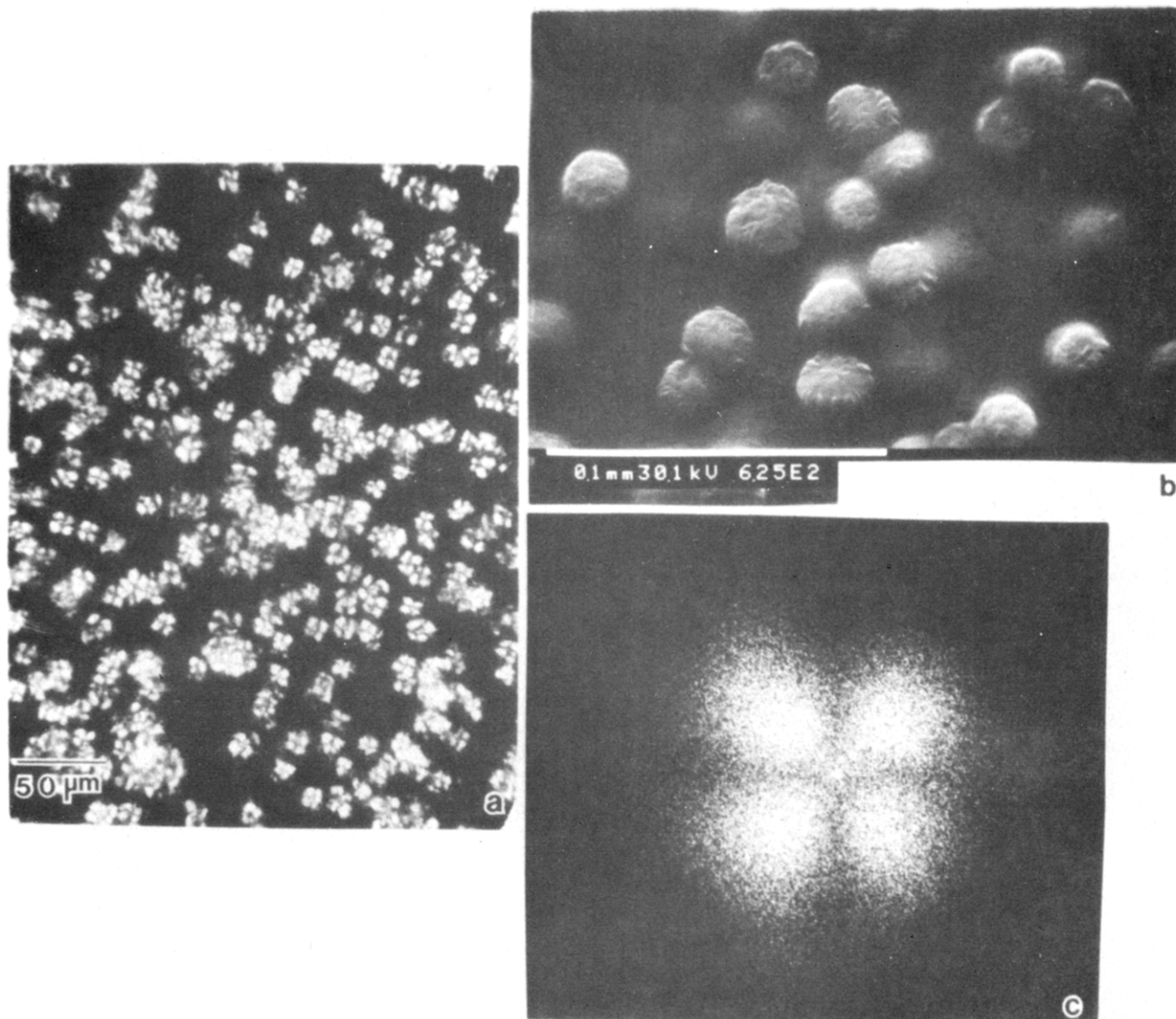


**Figure 2.** (a) Optical and (b) scanning electron micrographs of iPS film exposed to hexahydroindan vapor at ambient temperature for 10 days. The SALS pattern, in the  $H_v$  mode, is shown in c.

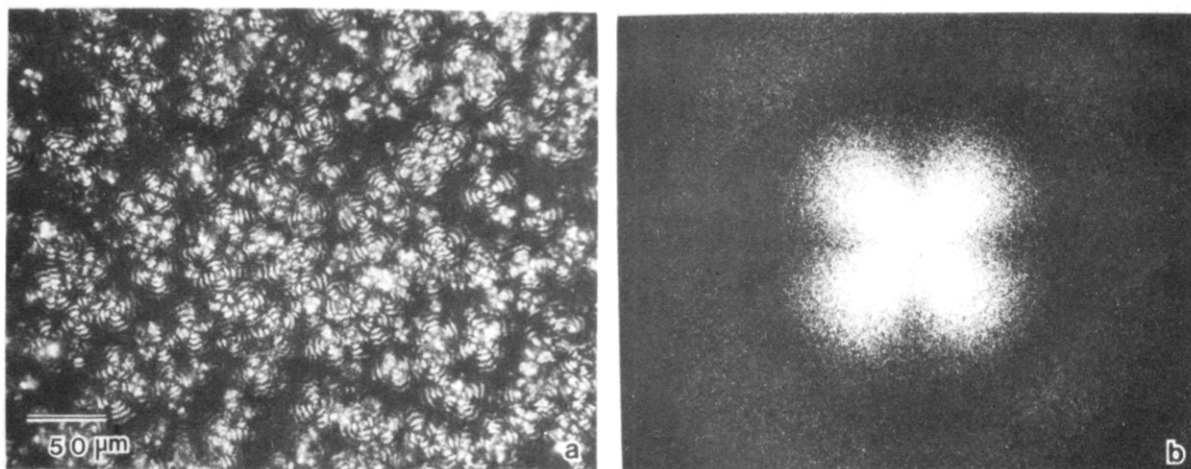


**Figure 3.** (a) Optical micrograph of iPS film exposed to cyclooctane vapor at ambient temperature for 14 days, showing ringed spherulitic morphology. (b) Corresponding SALS pattern in the  $H_v$  mode.

benzene, methylene chloride, acetone, hexahydroindan, and cyclooctane. These are known to promote crystallization of iPS. For SINC studies, the film was constrained in a circular steel frame and suspended above the solvent in the apparatus described before,<sup>2</sup> for specific periods of time. The apparatus was placed

in a thermostated bath. Following the removal from the solvent vapor, the films were dried at ambient conditions, in the constrained state.

The WAXD patterns were recorded by using a box-type flat film camera (William Warhus and Co.), with  $\text{Cu K}\alpha$  radiation ( $\lambda$

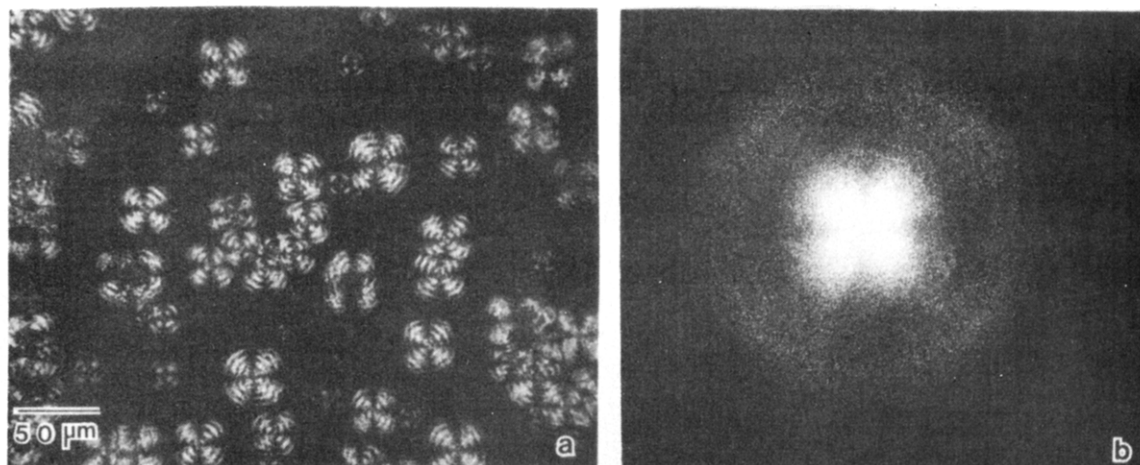


**Figure 4.** (a) Optical micrograph of iPS film exposed to cyclooctane vapor for 5 days, at 27 °C. (b) Corresponding SALS pattern in the  $H_v$  mode.

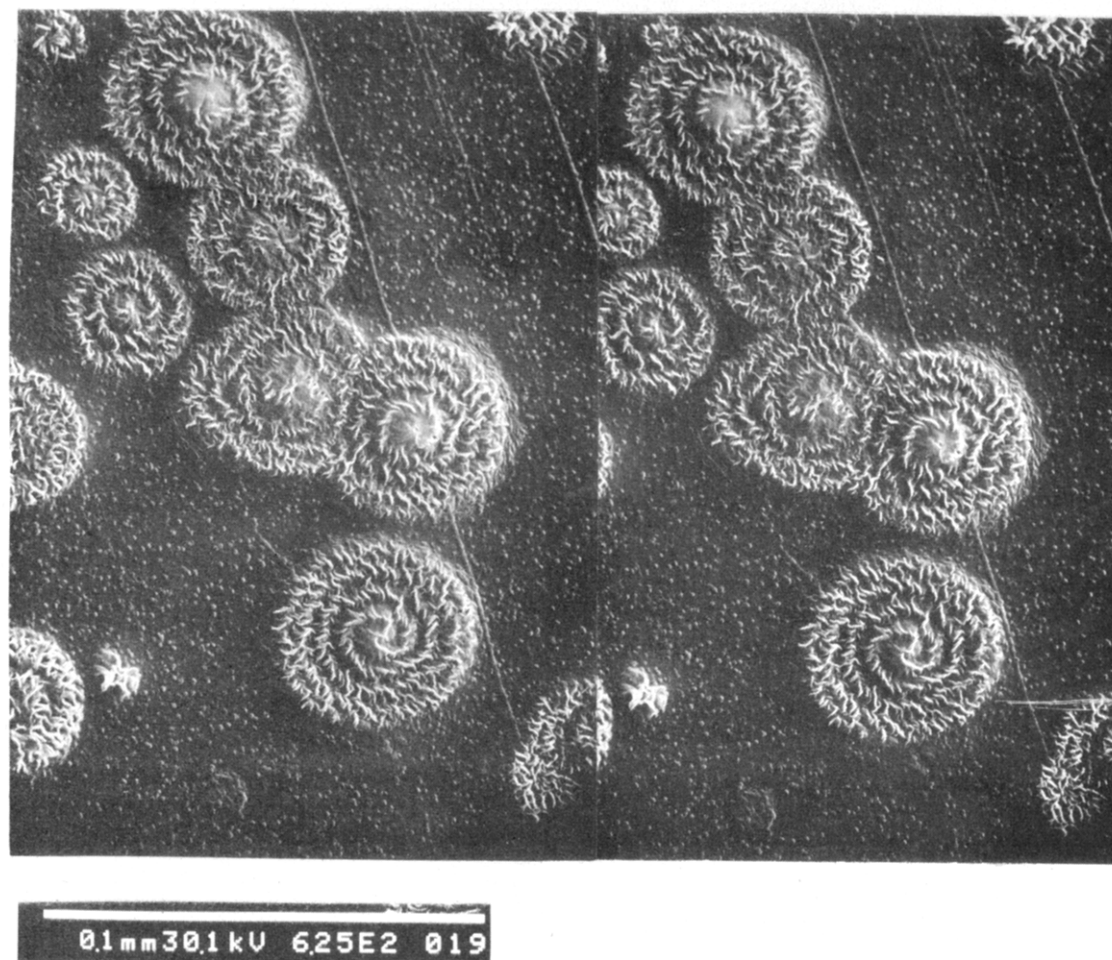


**Figure 5.** Stereoscopic SEM view of the sample used for Figure 4.

= 1.5418 Å). The SALS patterns were recorded on Polaroid films with a Spectra-Physics Model 115 He-Ne continuous gas laser source ( $\lambda = 6328$  Å). A Reichert polarizing optical microscope and a Philips 505 scanning electron microscope were used for microscopic studies. For the latter, the samples were coated, in the usual manner, with a thin layer of gold-palladium, to prevent sample charging. Stereoscopic images were obtained by recording two SEM micrographs of precisely the same area at two specimen tilt positions, separated by 5°.

## Results and Discussion

### Morphology as a Function of Duration of Vapor Exposure at Ambient Temperature. Typical SEM

micrographs of three different films of iPS, after exposure to hexahydroindan vapor for 30, 48, and 68 h, respectively, under ambient conditions, are shown in Figure 1. Several periods of exposure as above were chosen in order to characterize the various stages of growth of the spherulitic morphology. Detailed kinetic studies were not planned.

As the time of exposure increases from 30 to 68 h, the spherulitic characteristics become more pronounced. After 30 h of exposure (Figure 1a), ribbed ridges radiating from fibrillar spherulitic formations, about 10  $\mu\text{m}$  in diameter, are typical. The anisotropic spherulitic nature was verified with the polarizing OM. The corresponding X-ray diffraction pattern showed amorphous scattering, with a few



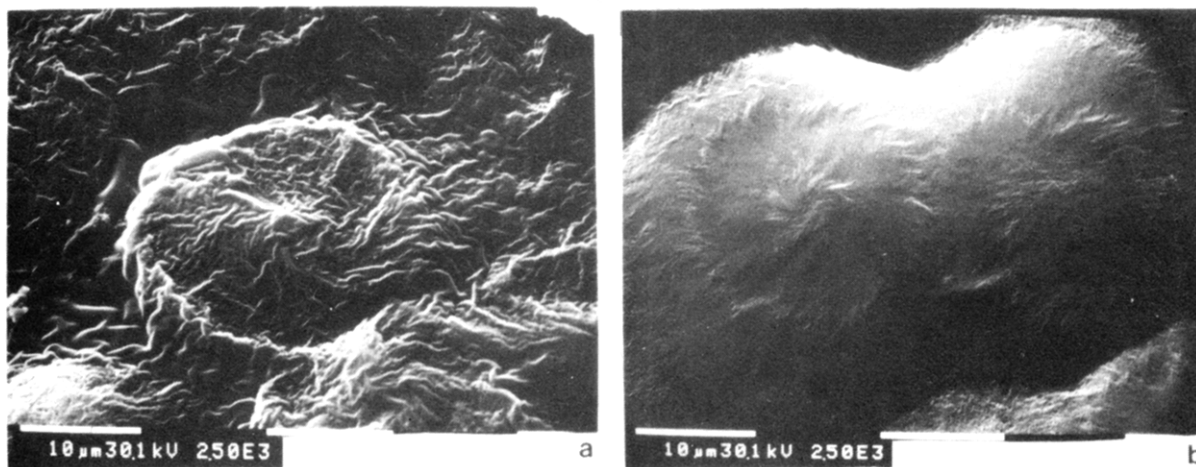


**Figure 6.** Scanning electron micrographs of iPS films exposed to (a) hexahydroindan and (b) cyclooctane vapor for 7 h at 30 °C.

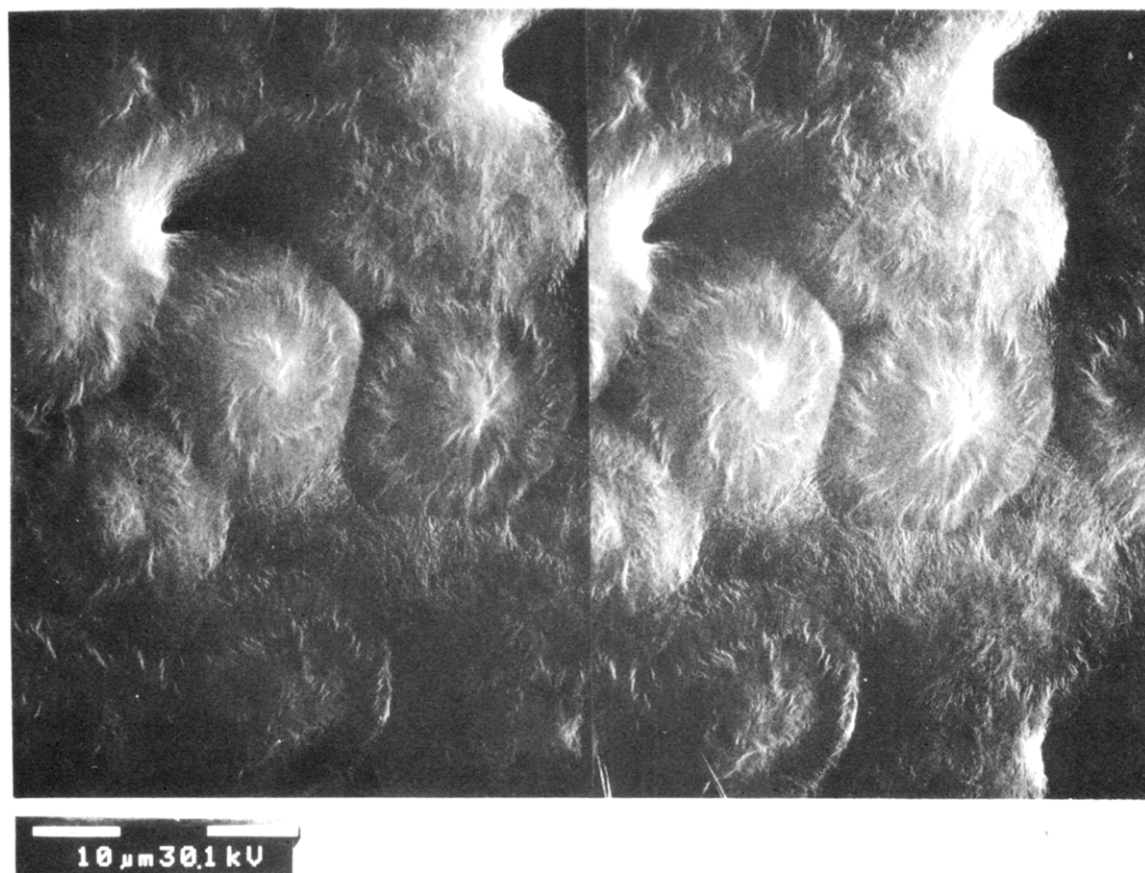


**Figure 7.** Stereoscopic view of the ringed spherulites obtained by exposing iPS film to cyclooctane vapor for 7 h at 30 °C.

faint reflections due to the  $\beta$  structure. After 48 h, the fibrillar texture becomes coarser and more pronounced (Figure 1b). Areas surrounding the spherulites show finer fibrillar branching. This is similar to the morphology described previously.<sup>1</sup> The X-ray diffraction pattern from this film showed reflections corresponding to the  $\beta$  form. Figure 1c shows the SEM micrograph, with well-formed discrete spherulites, following 68 h of exposure to the solvent vapor. These are nearly monodisperse in size, with an average diameter of  $\sim 20\ \mu\text{m}$ , and are positively birefringent. The spherulites are clustered together, with discrete boundaries but with no significant matrix material between them. Fine fibrillation is characteristic and at high magnification, shown in Figure 1d, the spherulites seem porous. The porosity could be due to solvent crazing.

Sharp reflections belonging to the  $\beta$  form were recorded in the X-ray pattern.

After 10 days of exposure to hexahydroindan vapor, the morphology shown in Figure 2 was obtained. The optical and SEM micrographs showed the morphology to be still spherulitic, but the spherulites are isolated. The transformation from the morphology seen in Figure 1c, where the spherulites are impinging with one another, to the one shown in Figure 2 does not find straightforward explanation. The decrease in the population of the spherulites cannot be attributed to "melting" caused by excess solvation, since there is no decrease in the size. The spherulites seen in Figure 2b show thin fibrillar texture and exhibit the typical four-leaf clover pattern (Figure 2c) in the  $H_v$  mode of SALS, with an average diameter of  $\sim 20$

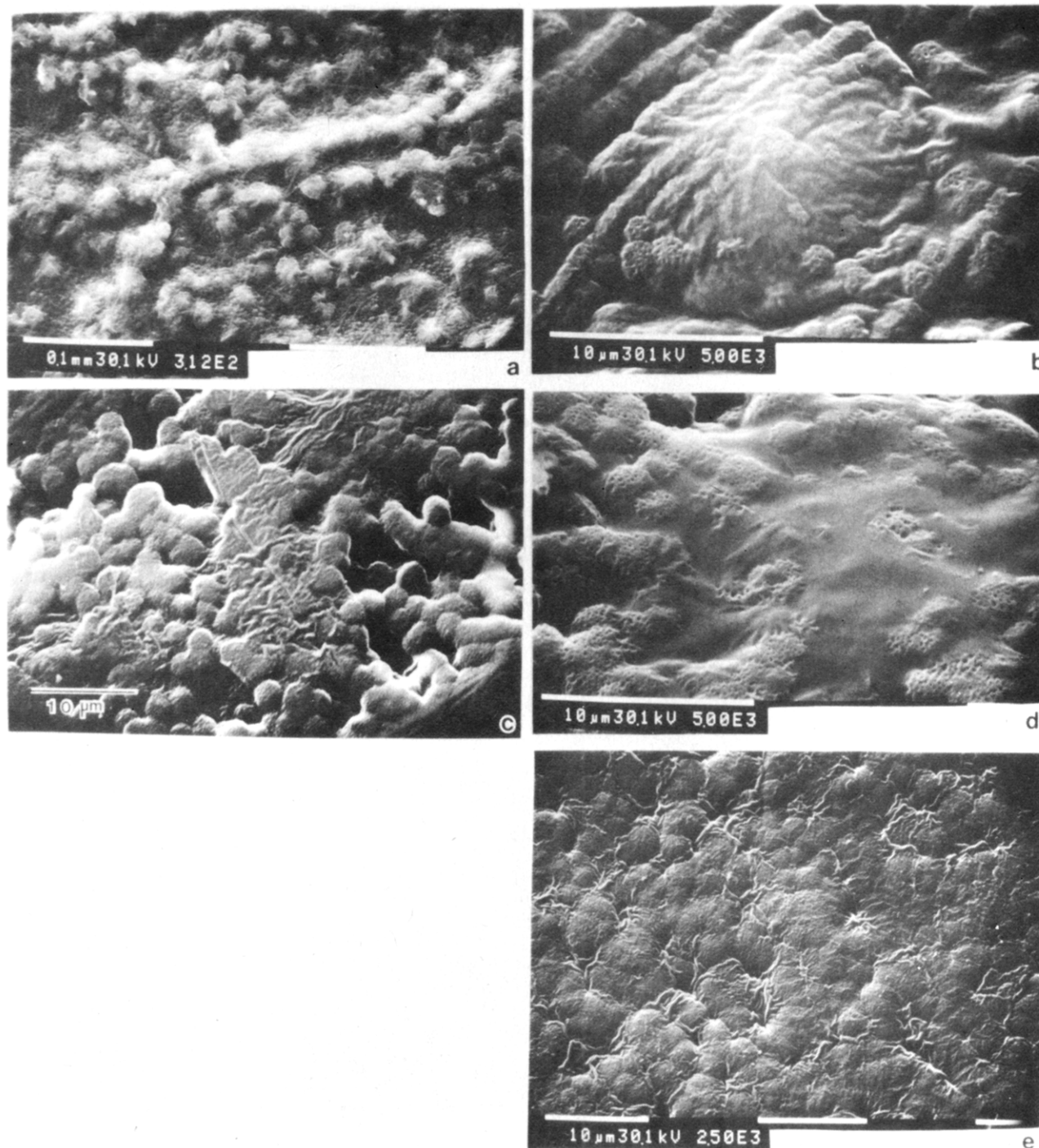


**Figure 8.** Scanning electron micrographs of iPS films exposed to hexahydroindan vapor at 35 °C for (a, b) 6 and (c) 19 h, (d) after annealing at 70 °C (see text), and (e) after 48 h.

$\mu\text{m}$ . The X-ray pattern confirmed the presence of the  $\beta$  structure but the possible crystallization of the  $\alpha$  form could not be identified unambiguously.

Figure 3 shows an optical micrograph and a SALS pattern of a film exposed to cyclooctane vapor at ambient conditions for 14 days. This solvent also promotes spherulitic morphology of the  $\beta$  structure, but in contrast to the case of hexahydroindan, these are ringed spherulites. There is no difference in the size of the spherulites, or their sign of birefringence, between the two cases. The SALS pattern (Figure 3b) in the  $H_v$  mode shows the four-leaf clover pattern and an additional maximum characteristic of ringed spherulites. The spacing of the rings was estimated to be 2–3  $\mu\text{m}$ . Reflections due to the  $\beta$  structure were predominant in the corresponding X-ray pattern.

**Exposure to Solvent Vapor above Ambient Temperatures.** Exposure of iPS film to cyclooctane vapor at 27 °C for 5 days also resulted in ringed spherulitic morphology. An optical micrograph and the corresponding SALS pattern are shown in Figure 4. A stereoscopic SEM view is shown in Figure 5. Figure 4a shows that there is a wide variation in the size of the spherulites, ranging from ~15 to 45  $\mu\text{m}$ . The ring spacing is about 3  $\mu\text{m}$  in all cases. Thus, the number of bands along the radius of the spherulites varies from 1 to 4, depending on the size of the latter. The SEM micrograph shows that some of the spherulites exhibit double-armed spirals, running counterclockwise, whereas the others are single spirals. Double-armed spirals of this type have been classically known in air-quenched thin films of linear polyethylene.<sup>8</sup>

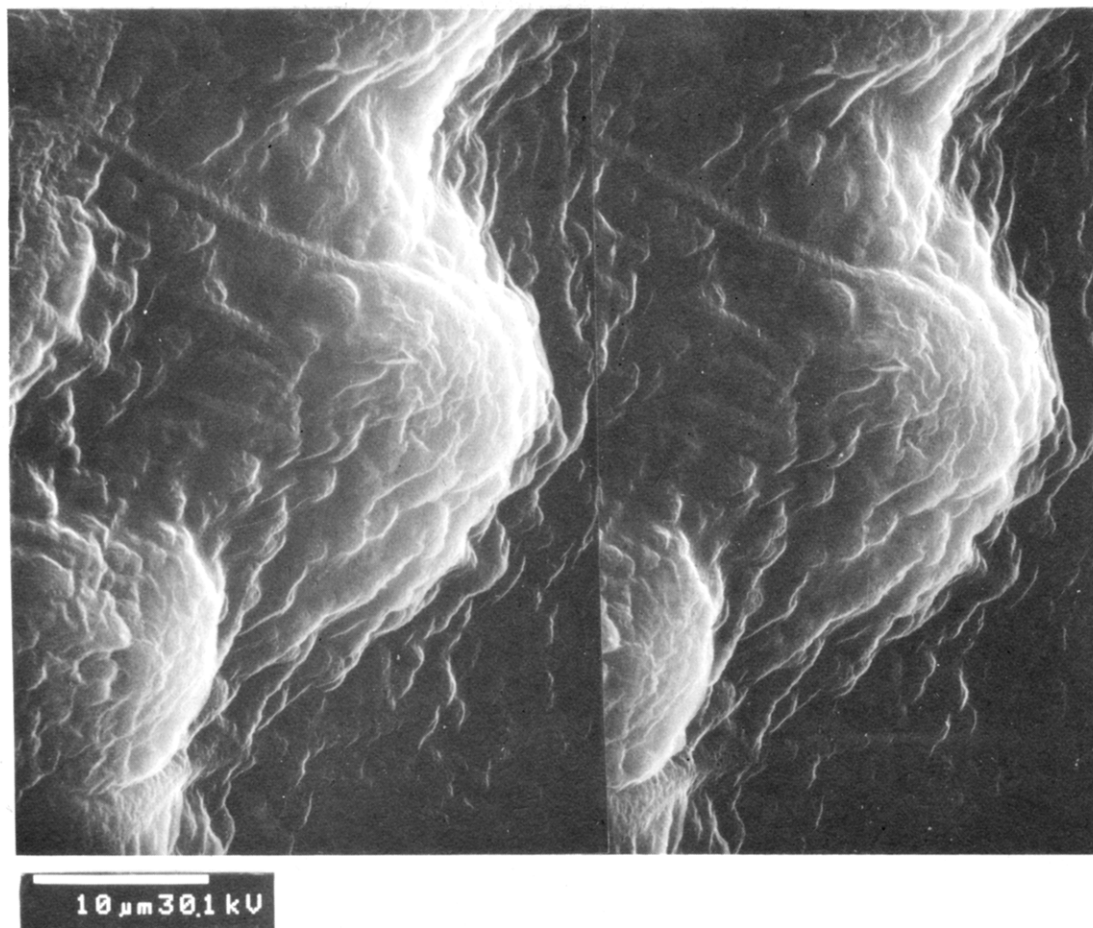


**Figure 9.** Stereoscopic view of the pincushion morphology obtained by exposing iPS film to hexahydroindan for 6 h at 35 °C.

The difference in the spherulitic texture induced by the two solvents is further illustrated in the SEM micrographs shown in Figure 6. Two films were exposed, one to hexahydroindan and the other to cyclooctane vapor, for 7 h, at 30 °C. The ringed spherulitic morphology, induced by cyclooctane vapor, is evident in Figure 6b. A stereoview of these spherulites is shown in Figure 7. The spherulites are  $\sim 30\ \mu\text{m}$  in diameter, with a ring spacing of  $\sim 5\ \mu\text{m}$ . Fine fibrils are seen in the ringed areas. In contrast, the spherulitic morphology caused by vapor exposure to hexahydroindan is extremely coarse, even when compared to the spherulites formed under ambient conditions (Figure 2b). The coarsening with increase in temperature of crystallization is consistent with the theory of spherulitic growth.<sup>9</sup> Apart from this, there appears to be no significant difference in either the size or the sign of birefringence of the spherulites, grown at this temperature, using either solvent. The X-ray patterns from both samples were similar, showing predominantly the reflections due to the  $\beta$  form, with a few faint reflections attributable to the  $\alpha$  form.

These results lead to the conclusion that the spherulites described above are due to the  $\beta$  structure. The electron diffraction result cited in the previous paper,<sup>2</sup> on thin sections of the samples used therein, also support this conclusion. In spite of the difference in the method of sample preparation and vapor exposure conditions, the overall morphology resulting in each case does not seem to be affected.

After exposure of amorphous, unoriented iPS film to hexahydroindan vapor, at 35 °C for 6 h, the WAXD pattern showed reflections due to the  $\beta$  structure as well as

the reflection with a spacing of 5.47 Å, characteristic of the  $\alpha$  form. The intensity of the latter was comparable to that of the 5.1-Å reflection of the  $\beta$  form. The SEM micrograph of this sample is shown in Figure 8a. Large spherulitic structures, of the order of 10–15  $\mu\text{m}$  in diameter, are seen with fibrillar texture. The cobweblike fibrillar formations crisscross in arbitrary directions. This feature has been observed before in the films of poly(ethylene terephthalate), crystallized by solvent vapor exposure.<sup>10</sup> The cobweb formation can perhaps be interpreted as follows: It is known that the amorphous materials in the films prepared by SINC show greater mobility than those in annealed films.<sup>11</sup> Since the films swell significantly upon vapor exposure, as the spherulitic crystallization takes place, parts of the sample between any two spherulites get dragged (or drawn) between them. Similar cobweb morphology has been seen in the case of nascent polyethylene, polymerized by using Zeigler catalysts.<sup>12–14</sup> It was explained on the basis that initial polymerization on the surface of the catalysts produces a crust around the catalyst conglomerates, and as the polymerization proceeds, the interior of the conglomerate expands, resulting in breakage of the polymer crust. The broken parts of the crust remain interconnected by the drawn fiber of the polymer. It was also found in these studies on nascent morphology that similar cobweb morphology does not occur in the polymerization of polypropylene and this was attributed to the slow rate of polymerization.<sup>12,13</sup> Drawing a parallel, it is possible that the cobweb morphology observed in the SINC arises when the crystallization is rapid. It should be noted that the morphology shown in Figure 8a was obtained after 6 h of exposure to the vapor, com-

pared to longer times of exposure at room temperature.

In addition, as seen in higher magnification shown in Figure 8b, the large spherulites contain smaller spherulitic overgrowths, almost resembling a pincushion. The small spherulites, about 1–2  $\mu\text{m}$  in size, are seen in the matrix surrounding the large spherulites as well, and are porous. A stereoview of the pincushion morphology is shown in Figure 9. The large spherulites have been identified with the  $\beta$  form and the smaller ones with the  $\alpha$ , as shown below. The ribbonlike texture, crisscrossing in arbitrary directions, can be attributed to the stress caused by the swelling during solvent exposure and subsequent contraction upon drying.

The WAXD pattern from the film exposed to hexahydroindan vapor at 35 °C, for 19 h, showed intense reflections due to the  $\alpha$  structure, along with faint ones from the  $\beta$  form. In the SEM micrograph, shown in Figure 8c, the small spherulites predominate, while the large ones have lost clarity, giving a smeared-out appearance. In order to definitively associate the large spherulites with the  $\beta$  form, the film used for obtaining the WAXD pattern was annealed at 70 °C (above the  $T_m$  of the  $\beta$  structure crystallized with this solvent). The WAXD pattern showed that the  $\beta$  form had melted. Figure 8d shows the SEM micrograph of the annealed film. While the small spherulites remain unaffected, the region once occupied by the large spherulite is now smooth and featureless. This confirms that the large spherulites correspond to the  $\beta$  structure.

After 48 h of exposure, at the same temperature, the WAXD pattern showed reflections due to the  $\alpha$  form, and those due to the  $\beta$  form were hardly detectable. The SEM micrograph (Figure 8e) shows the small spherulites, with a few fibrillar zones between them. Finally, after 6 days of vapor exposure, the fibrillar texture was absent and only the small spherulites, characteristic of the  $\alpha$  form, were observed.

Exposure at 30 °C for various periods of time produced similar results, except that after 9 days of exposure, the  $\beta$  form was still present. Thus, the temperature and duration of exposure to the solvent vapor have a combined effect on the cocrystallization and the resulting morphology. It has not been possible, in our attempts so far, to obtain similar pincushion morphology in films exposed to cyclooctane vapor.

## Conclusions

The various stages of development of the spherulitic structures in iPS films have been examined. The duration of exposure has an influence on the texture as well as upon which polymorph(s) crystallizes. Prolonged exposures above ambient temperatures cause excess solvation and result in the "melting" of the  $\beta$  structure. The results obtained here in terms of the proportion of the two crys-

talline components cannot be directly related to the previous results on melt-quenched starting films.<sup>2</sup> The tacticity and the film-preparation method are different in the two cases. The overall similarity of the morphology obtained is striking, however. The exposure to cyclooctane vapor results in ringed spherulitic morphology with both melt-quenched and toluene-cast starting films. The differences in the details of the morphologies obtained here and those reported previously indicate that the starting material (its molecular weight, tacticity, etc.) and the conditions of vapor exposure have an influence on the resulting morphology. We have confined to the case of vapor exposure rather than immersion in the liquid.

Although spherulitic growth is commonly observed in the SINC of polymers, the pincushion type of overgrowth of small spherulites ( $\alpha$  form) on the larger ones ( $\beta$  form) is a new morphological feature. This would indicate that the  $\beta$  structure perhaps acts as nucleating sites for the crystallization of the  $\alpha$  form. Recent TEM studies<sup>7</sup> on the gels of iPS show that this is indeed the case. In addition to the ringed spherulitic morphology, the double- and single-armed spirals are also new features in the SINC area. Sorting and understanding the factors which govern these ultimate morphologies would doubtless be rewarding in characterizing the process of SINC in a system such as isotactic polystyrene.

**Registry No.** iPS (homopolymer), 25086-18-4.

## References and Notes

- (1) Sundararajan, P. R.; Tyrer, N. J. *Macromolecules* **1982**, *15*, 1004.
- (2) Tyrer, N. J.; Bluhm, T. L.; Sundararajan, P. R. *Macromolecules* **1984**, *17*, 2296.
- (3) Atkins, E. D. T.; Isaac, D. H.; Keller, A.; Miyasaka, K. *J. Polym. Sci., Polym. Phys. Ed.* **1977**, *15*, 211.
- (4) Sundararajan, P. R.; Tyrer, N. J.; Bluhm, T. L. *Macromolecules* **1982**, *15*, 286.
- (5) Hill, M. J.; Barham, P. J.; Keller, A. *Colloid Polym. Sci.* **1983**, *261*, 721.
- (6) Buleon, A.; Chanzy, H.; Roche, E. *J. Polym. Sci., Polym. Phys. Ed.* **1976**, *14*, 1913; *J. Polym. Sci., Polym. Lett. Ed.* **1977**, *15*, 265.
- (7) Atkins, E. D. T.; Hill, M. J.; Jarvis, D. A.; Keller, A.; Sarhene, E.; Shapiro, J. S. *Colloid Polym. Sci.* **1984**, *262*, 22.
- (8) Geil, P. H. "Polymer Single Crystals"; R. E. Kreiger Publishing Co.: New York, 1973; p 244.
- (9) Wunderlich, B. "Macromolecular Physics"; Academic Press: New York, 1973; Vol. 1, p 324.
- (10) Makarewicz, P. J. Ph.D Thesis, Princeton University, Princeton, NJ, 1977, p 44.
- (11) Zachmann, H. G. *Makromol. Chem.* **1964**, *74*, 29. Eichhoff, V.; Zachmann, H. G. *Ibid.* **1971**, *147*, 40.
- (12) Graff, R. J. L.; Kortleve, G.; Vonk, C. G. *J. Polym. Sci., Part B* **1970**, *8*, 735.
- (13) Marchessault, R. H.; Fisa, B.; Chanzy, H. D. *CRC Crit. Rev. Macromol. Sci.* **1972**, *1*, 315.
- (14) Chanzy, H. D.; Revol, J. F.; Marchessault, R. H.; Lamande, A. *Kolloid. Z. Polym.* **1973**, *251*, 563.